Mechanical properties of suspended graphene sheets

I. W. Frank and D. M. Tanenbaum[a)]
Pomona College, Department of Physics and Astronomy, Claremont, California 91711

A. M. van der Zande and P. L. McEuen
Cornell Center for Materials Research, Cornell University, Ithaca, New York 14853

(Received 10 June 2007; accepted 27 August 2007; published 11 December 2007)

Using an atomic force microscope, we measured effective spring constants of stacks of graphene sheets (less than 5) suspended over photolithographically defined trenches in silicon dioxide. Measurements were made on layered graphene sheets of thicknesses between 2 and 8 nm, with measured spring constants scaling as expected with the dimensions of the suspended section, ranging from 1 to 5 N/m. When our data are fitted to a model for doubly clamped beams under tension, we extract a Young's modulus of 0.5 TPa, compared to 1 TPa for bulk graphite along the basal plane, and tensions on the order of 10^{-7} N. © *2007 American Vacuum Society.* [DOI: 10.1116/1.2789446]

I. INTRODUCTION

Nanoelectromechanical systems (NEMSs) have many applications in fundamental science and engineering, such as the study of quantum limited motion,[1] mass detection,[2,3] and force detection.[4] In all of these applications, it is extremely beneficial to have the active element have as low of a mass as possible and as high of a quality factor as possible.[5] Materials such as Si, SiO_2 SiN, SiC, diamond, and GaAs have been studied with the prototypical resonator consisting of a nanoscale beam clamped on one or both ends.[6] Graphite appears to be an excellent material for the fabrication of NEMS resonators. Its makeup of strongly bonded planar sheets held together by weak van der Waals interactions makes it relatively simple to fabricate extremely thin resonators, even down to the natural limit of one atomic layer. Graphene, like carbon nanotubes, is extremely strong and stiff compared to silicon based materials. Beyond its material strength, graphene is advantageous due its tunable electronic properties, chemical inertness, and high thermal conductivity.[7]

Before suspended graphene sheets can become the basis for any practical NEMS sensors, their mechanical properties must be measured as they may deviate from the known properties of the bulk graphite. Using atomic force microscopy (AFM), we are able to accurately measure the length, width, and thickness of suspended stacks of graphene sheets. By pressing on the suspended sheets with AFM tips with calibrated spring constants, we are able extract the spring constants of the sheets. By examining how the spring constants vary with the size dimensions of the suspended sheets, we are able to extract built-in axial tensions and the Young's modulus of the graphene layers.

II. BACKGROUND

We have previously reported that suspended graphene sheets can be resonated in vacuum[8] with an optical detection setup using either a modulated blue laser that locally heats the sample,[3] or a capacitive drive using a varying potential between the silicon backplane and the suspended graphite.[9] This dynamic method allows for highly accurate measurements of the resonant frequencies, but it is nontrivial to determine the absolute amplitude of the motion. While this can be accomplished by examining the thermal noise, it is not a direct measurement and the calibration is different each time a sample is mounted in the detection system. In contrast, static AFM deflection measurements provide a simple and direct measurement of both displacement and force for the determination of spring constants.

In our previous work on dynamic measurements, we modeled the resonators as doubly clamped beams in the limit of small tension.[8] As was noted in this work, it is likely that tension matters, particularly for the thinnest samples. The equation determining the fundamental natural frequency (hertz) of a doubly clamped beam under tension is

$$f = 1.03\sqrt{\frac{Et^2}{\rho L^4} + \frac{T}{3.4mL}}, \tag{1}$$

where T is the tension in the beam, E is the Young's modulus, ρ is the density of the material, m is the effective mass, and t and L are the thickness and length of the beam, respectively. The numerical constants are determined by clamping conditions.[10,11] Using the relation $f=(1/2\pi)\sqrt{k/m}$, where k is the effective spring constant of the beam, we can solve for k. The resulting equation is

$$k = 30.78Ew(t/L)^3 + 12.32(T/L), \tag{2}$$

where w is the width of the beam.

In the case of static deflection measurements, the distribution of the load is from a point contact rather than along the beam as in the dynamic measurements of resonators. Thus, while the functional form is the same with contributions from both bending and tension, the constants are not. For a doubly clamped beam in equilibrium with a static force applied at the center of the beam and under axial tension, the resulting equation is

a)Electronic mail: dtanenbaum@pomona.edu

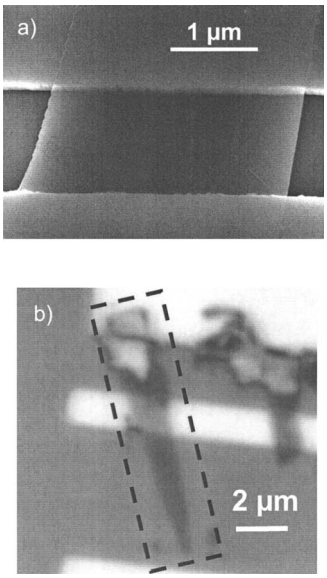

FIG. 1. (a) A SEM micrograph of a graphene sheet suspended above a trench (horizontal stripe) etched in silicon dioxide. The sheet measured 7 nm thick by AFM. (b) An optical micrograph of a different suspended few-layer graphene sheet measured to be 2 nm thick by AFM.

$$k = 16.23Ew(t/L)^3 + 4.93T/L. \quad (3)$$

This expression holds until the deflection moves beyond the linear regime in Hooke's law due to the stretching of the beam.[12,13]

III. FABRICATION AND YIELD

Suspended stacks of graphene are obtained by mechanically exfoliating kish graphite[14] across photolithographically patterned trenches that act analogous to a cheese grater and shear off thin sheets of the graphite.[8,15–18] The graphite sheets can be up to 50 nm thick and as thin as a single layer of atoms. Their length and width are largely determined by the size of the trenches and are generally between 0.5 and 5 μm. Kish graphite comes in flakes that are a few millimeters on a side. These flakes are then attached to a probe which acts as a "pencil." The graphite is cleaved, exposing an atomically smooth surface on the tip of the pencil. The pencil is then rubbed across the silicon oxide substrate, mechanically exfoliating pieces of graphite onto the surface.

The key to this production technique is in selecting the thickness of the dielectric that the sheets of graphite are resting on. With the correct thickness of the oxide (280 nm as measured by thin film interferometry), the very thin suspended graphene sheets show up in vivid shades of purple in an optical microscope.[19] The hue of the graphite can be correlated with its thickness and allows for a quick determination of graphene sheets, meriting further characterization with an AFM. Figures 1(a) and 1(b) are a scanning electron microscope (SEM) and an optical micrograph of suspended graphene sheets, respectively.

Once the desired pieces have been selected optically, more accurate measurements are performed with an AFM (Ref. 20) in ac mode to provide the width and length of the suspended graphite with nanometer resolution. AFM was used in ac mode to image the suspended graphene sheets as it is less likely to cause damage than contact mode. For sheets thinner than 2–3 nm, the measurement of the thickness with AFM is unreliable for determining the number of graphene layers so Raman spectroscopy is used to get an accurate count.[21–23]

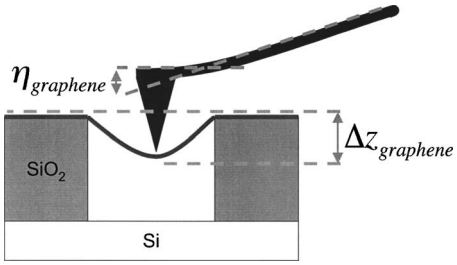

FIG. 2. A schematic of an AFM tip that is deflected while pushing down on a suspended graphene sheet. η_{graphene} is measured by the AFM and $\Delta z_{\text{graphene}}$ is calculated using Eq. (4).

In contrast to the fabrication of oscillators made from suspended carbon nanotubes that display significant slack,[9] all the suspended graphene sheets made via exfoliation appear to be under tension. This tension can be increased by applying a dc bias between the suspended graphite and the silicon backplane which can be used to tune the resonance frequency of the suspended graphene layers.[8,9]

IV. STATIC DEFLECTION MEASUREMENTS

Static deflection measurements are made by acquiring force distance curves with an AFM. Once the dimensions of the suspended graphene layers have been measured by AFM, the tip is pushed down in the center of the beam in ac mode, and both amplitude and deflection signals are recorded versus z_{piezo}.[24,25] Figure 2 is a schematic of an AFM tip pushing down on suspended graphene layers. From the deflection of the tip as it pushes down on the suspended sheet, we are able to extract the effective spring constant (k) of the suspended graphene layers. It is important that the spring constant of the tip be close to that of the graphite sheets or an accurate measurement becomes impossible. If the tip is too stiff in comparison to the graphene layers, it will not deflect a detectable amount. If the tip is too soft, the sheets will appear to be rigid and no meaningful information can be extracted from the measurement. We used tips with a nominal spring constant of 2 N/m.[26] These are 240 μm long silicon cantilevers designed for ac mode. Each tip's spring constant is individually calibrated using a reference cantilever with a known spring constant.[27] The calibration process involves comparing the results of pushing the AFM tip against an immovable surface and the reference cantilevers, following the approach of Tortonese and Kirk.[28] Once the spring constant of the tips are known, the suspended graphene sheet's spring constant can be measured. The tip is pushed slowly ($\sim$100 nm/s) against the sheets in order to minimize damage to the tip and the graphite, and a curve of the tip displacement versus the position of the piezo is obtained [see Fig.

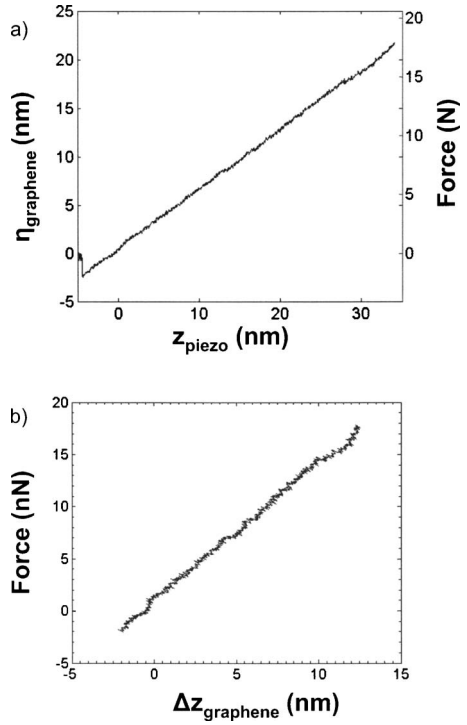

FIG. 3. (a) On the left axis is the curve obtained by the AFM while pushing down on a suspended graphene sheet. The right axis is the corresponding force. (b) Graph of force vs displacement of the suspended sheet. The spring constant of the sheet is the slope of these data.

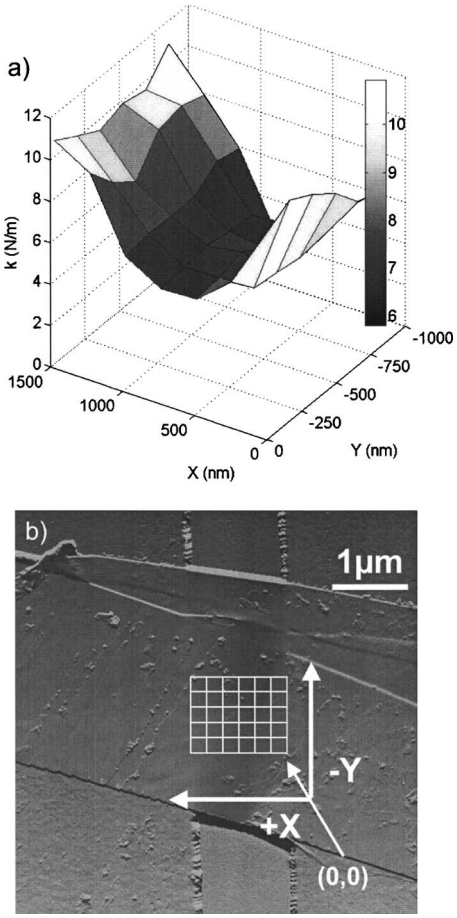

FIG. 4. (a) A surface plot of the spring constant of a suspended graphene sheet vs the location of the AFM tip. (b) An amplitude AFM micrograph of the suspended sheet measured to obtain (a) and imaged in by SEM in Fig. 1(a). Each data point was taken at the intersection of the grid located on the suspended portion of the graphene. The trench etched into the silicon dioxide is seen as a vertical stripe.

3(a)]. As the AFM tip comes into contact with the suspended graphene device, the free amplitude of the ac motion of the tip cantilever goes to zero, and the cantilever is pulled down onto the surface, resulting in the initial dip in the deflection seen in Fig. 3(a). Using our measured spring constant of the tip, we are able to extract a graph of the force exerted on the tip versus the displacement of the graphene sheets [see Fig. 3(b)]. We calculate the displacement using

$$z_{\text{piezo}} = \eta_{\text{graphene}} + \Delta z_{\text{graphene}}, \tag{4}$$

where η_{graphene} is the deflection of the tip measured by the AFM, z_{piezo} is location of the piezos moving the tip, and $\Delta z_{\text{graphene}}$ is the deflection of the suspended layers of graphene. In the regime of small displacements—on the order of the thickness of the layers—this curve will be linear [see Fig. 3(b)] and through Hooke's law the slope will yield the effective spring constant of the suspended graphene sheets. Using this technique, we measured spring constants of $1-5\ \text{N/m}$ in suspended sheets with thicknesses from 2 to 8 nm.

It is an interesting question how the spring constant changes over the length and width of the sheet, and what can be termed the center of the beam, especially since many of the sheets are of trapezoidal shape with slightly varying thicknesses across the suspended portion. Some spatial scans of the sheets, an example of which is displayed in Fig. 4(a), measuring the spring constant at various points, show that the spring constant of the suspended sheets rises by over a factor of 2 nearer the clamped edges and falls of slightly nearer the free edges, making a saddle point of the spring constant in the center. However, in the center, the effect is fairly small; so long as the tip is within 100 nm of the center of a 1 μm long suspended sheet, the spring constant is set within the reproducibility of the measurements.

V. DISCUSSION

In Fig. 5 we plot spring constants for eight different suspended graphene sheets versus the quantity $w(t/L)^3$, the dependence of the directly measured quantities in the bending term, from Eq. (3). Although the tension term in Eq. (3) is important for our suspended graphene sheets, we note that L was similar in all the sheets we measured and the $w(t/L)^3$ term is expected to vary much more than the T/L term. As a result, in our analysis we model the T/L term as a constant offset to a linear fit of k vs $w(t/L)^3$. This assumes that all the sheets have similar tensions; however, given the linear nature of our data, plotted in Fig. 5, this appears to be a good approximation.

Figure 5 shows that one of our 2 nm thick graphene sheets does not fall near our linear fit of all the data shown as

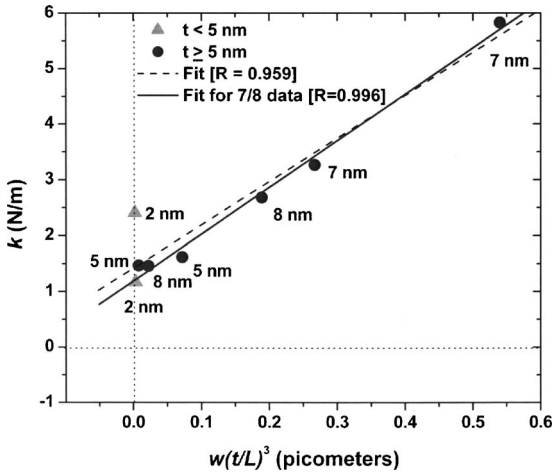

FIG. 5. A plot of the spring constant as measured in the center of the suspended region of the graphene sheets, vs $w(t/L)^3$ for eight different samples. From the linear fit, we are able to extract an average tension and a Young's modulus. The dashed line is the fit to all the data points, whereas the solid line is the fit for 7/8 of the data.

a dashed line in Fig. 5. This could be due to many factors including the unusually high tension, loss of rigidity in the beam, or different clamping conditions. As a result, we focus our discussion on the measurements made on the remaining seven data points fitted as the solid line in Fig. 5. The slope of this solid line suggests an E of 0.5 TPa, compared to the 1 TPa value for bulk graphite.[7] Using the offset of the linear fit and an average L, we obtain a tension of 300 nN, suggesting that the tension in all the sheets is on the order of hundreds of nanonewtons. Calculations with each individual device's length suggest this to be accurate.

VI. CONCLUSION

We have performed static and dynamic measurements of the mechanical properties of nanometer-thick suspended graphite sheets made by exfoliating thin layers of graphite over trenches patterned in silicon dioxide films on a silicon substrate. We present a simple, direct, and nondestructive approach for obtaining the mechanical properties of atomically thin membranes with AFM. In contrast to other techniques, this approach has spatial resolution on the nanometer scale and can map properties across a membrane. In contrast to NEMS based on molecules such as DNA and carbon nanotubes, membranes of graphene can be used as barriers between different environments, and the technique presented can be adapted to work in vacuum or fluid cells. Spring constants ranging from 1 to 5 N/m were observed for suspended graphene sheets less than 10 nm thick. Fitting to the model of a doubly clamped beam in equilibrium with a static force and under axial tension, we extracted a Young's modulus of 0.5 TPa, significantly below the bulk value of 1 TPa, and tensions of hundreds of nanonewtons. For one of our eight sheets, the behavior is erratic and is only a loose fit to our model.

ACKNOWLEDGMENTS

The authors would like to thank the NSF for support through the Cornell Center for Materials Research, the Cornell Center for Nanoscale Systems, and the Cornell Nano-Scale Facility, a member of the National Nanotechnology Infrastructure Network. Additionally the authors would like to thank Leon Bellan, Scott Bunch, Scott Verbridge, Scott Berkley, Jeevak Parpia, and Harold Craighead for helpful discussions and support.

[1] M. LaHaye, O. Buu, B. Camarota, and K. Schwab, Science **304**, 74 (2004).
[2] K. Ekinci, Y. Yang, and M. Roukes, J. Appl. Phys. **95**, 2682 (2004).
[3] B. Ilic, J. Appl. Phys. **95**, 3694 (2004).
[4] D. Rugar, R. Budakian, H. Mamin, and B. Chui, Nature (London) **430**, 329 (2004).
[5] H. Craighead, Science **290**, 1532 (2000).
[6] K. Ekinci and M. Roukes, Rev. Sci. Instrum. **76**, 061101 (2005).
[7] B. Kelly, *Physics of Graphite* (Applied Science, Englewood, NJ, 1981).
[8] J. S. Bunch, A. M. van der Zande, S. S. Verbridge, I. W. Frank, D. M. Tanenbaum, J. M. Parpia, H. G. Craighead, and P. L. McEuen, Science **315**, 490 (2007).
[9] V. Sazonova, Y. Yaish, H. Uestuenel, D. Roundy, T. A. Arias, and P. L. McEuen, Nature (London) **431**, 284 (2004).
[10] S. C. Jun, X. Huang, M. Manolidis, C. Zorman, M. Mehregany, and J. Hone, Nanotechnology **17**, 1506 (2006).
[11] W. Weaver, S. P. Timoshenko, and D. H. Young, *Vibration Problems in Engineering*, 5th Ed. (Wiley, New York, 1990), p. 454.
[12] M. W. Pruessner, T. T. King, D. P. Kelly, R. Grover, L. C. Calhoun, and R. Ghodssi, Sens. Actuators, A **105**, 190 (2003).
[13] S. D. Senturia, *Microsystem Design* (Kluwer Academic, Boston, MA, 2000), p. 249.
[14] Purchased from Toshiba Ceramics.
[15] J. S. Bunch, Y. Yaish, M. Brink, K. Bolotin, and P. L. McEuen, Nano Lett. **5**, 287 (2005).
[16] K. Novoselov, D. Jiang, F. Schedin, T. Booth, V. Khotkevich, S. Morozov, and A. Geim, Proc. Natl. Acad. Sci. U.S.A. **102**, 10451 (2005).
[17] K. S. Novoselov, A. K. Geim, S. V. Morozov, D. Jiang, M. I. Katsnelson, I. V. Grigorieva, S. V. Dubonos, and A. A. Firsov, Nature (London) **438**, 197 (2005).
[18] Y. Zhang, Y. W. Tan, H. L. Stormer, and P. Kim, Nature (London) **438**, 201 (2005).
[19] P. Blake, K. Novoselov, A. H. C. Neto, D. Jiang, R. Yang, T. Booth, A. Geim, and E. Hill, Appl. Phys. Lett. **91**, 063124 (2007).
[20] We used a Dimension 3000 AFM from Digital Instruments.
[21] A. C. Ferrari, J. C. Meyer, V. Scardaci, C. Casiraghi, M. Lazzeri, F. Mauri, S. Piscanec, D. Jiang, K. S. Novoselov, S. Roth, and A. K. Geim, Phys. Rev. Lett. **97**, 187401 (2006).
[22] A. Gupta, G. Chen, P. Joshi, S. Tadigadapa, and P. C. Eklund, Nano Lett. **6**, 2667 (2006).
[23] D. Graf, F. Molitor, K. Ensslin, C. Stampfer, A. Jungen, C. Hierold, and L. Wirtz, Nano Lett. **7**, 238 (2007).
[24] J. D. Whittaker, E. D. Minot, D. M. Tanenbaum, P. L. McEuen, and R. C. Davis, Nano Lett. **6**, 953 (2006).
[25] E. Minot, Y. Yaish, V. Sazonova, J. Y. Park, M. Brink, and P. L. McEuen, Phys. Rev. Lett. **90**, 156401 (2003).
[26] Olympus AC-240TS.
[27] Purchased from Veeco Metrology; calibration performed with Laser Doppler Vibrometry by B.Ohler as per Application Note 94, Veeco Instruments, Inc. (2007).
[28] M. Tortonese and M. Kirk, Proc. SPIE **3009**, 53 (1997).